

Prototyping and Experimental Results for Environment-Aware Millimeter Wave Beam Alignment via Channel Knowledge Map

Zhuoyin Dai, Di Wu, Zhenjun Dong, Kun Li, Dingyang Ding,

Sihan Wang, and Yong Zeng, *Senior Member, IEEE*

Abstract—Channel knowledge map (CKM), which aims to directly reflect the intrinsic channel properties of the local wireless environment, is a novel technique for achieving environment-aware communication. In this paper, to alleviate the large training overhead in millimeter wave (mmWave) beam alignment, an environment-aware and training-free beam alignment prototype is established based on a typical CKM, termed beam index map (BIM). To this end, a general CKM construction method is first presented, and an indoor BIM is constructed offline to learn the candidate transmit and receive beam index pairs for each grid in the experimental area. Furthermore, based on the location information of the receiver (or the dynamic obstacles) from the ultra-wide band (UWB) positioning system, the established BIM is used to achieve training-free beam alignment by directly providing the beam indexes for the transmitter and receiver. Three typical scenarios are considered in the experiment, including quasi-static environment with line-of-sight (LoS) link, quasi-static environment without LoS link and dynamic environment. Besides, the receiver orientation measured from the gyroscope is also used to help CKM predict more accurate beam indexes. The experiment results show that compared with the benchmark location-based beam alignment strategy, the CKM-based beam alignment strategy can achieve much higher received power, which is close to that achieved by exhaustive beam search, but with significantly reduced training overhead.

Index Terms—Channel knowledge map, environment-aware communication, training-free beam alignment, millimeter wave.

I. INTRODUCTION

Millimeter wave (mmWave) massive multiple-input multiple-output (MIMO) is an effective technology to meet the ever-increasing capacity requirement for the fifth-generation (5G) and beyond mobile communication networks [1]–[3]. On the one hand, the mmWave band at 26.5–300 GHz has abundant spectrum, which can effectively alleviate the spectrum crunch issue. On the other hand, the short wavelengths at mmWave frequencies allow more antennas to be compactly packed at the transmitter and receiver to compensate for the path loss. Although large antenna arrays bring considerable beamforming gains, the overall system overhead also increases significantly, not only in

The authors are with the National Mobile Communications Research Laboratory, Southeast University, Nanjing 210096, China. Y. Zeng is also with the Purple Mountain Laboratories, Nanjing 211111, China (e-mail: {zhuoyin_dai, studywudi, zhenjun_dong, 220205571, 220200693, turquoise, yong_zeng}@seu.edu.cn). (Corresponding author: Yong Zeng.)

terms of the hardware cost, but also the high overhead to practically achieve the large-dimensional beamforming gain. Some cost-effective techniques have been proposed for mmWave massive MIMO communication. For example, hybrid analog/digital beamforming has been extensively studied to reduce the cost of radio frequency (RF) chains [4]–[7], where signal processing is divided into the digital domain and analog domain. Deploying low-precision digital-to-analog converters (ADC) is also a possible way to reduce hardware costs and power consumption in mmWave systems [8]. Lens antenna array is another cost-effective mmWave communication technology, which utilizes electromagnetic lenses to separate signals from different directions without requiring sophisticated signal processing [9]–[12].

It is important to note that the radio propagation environment has a significant effect on the performance of communication systems. In practice, it is typically necessary to acquire real-time channel state information (CSI) to completely realize the performance gain of highly directional beamforming. To this end, one major approach is to use training-based CSI estimation for beamforming design [7], [13], [14]. However, for cost-effective implementations such as hybrid beamforming, the increasing size of antennas may significantly increase the overhead for CSI acquisition, since the channel measured in the digital baseband is entangled with the analog beamforming for training. An alternative beamforming method for mmWave massive MIMO is training-based beam sweeping [15]–[18]. Instead of estimating the MIMO channels for beam selection, this method sequentially sweeps the beamforming vectors in the predefined codebook to find the optimal transmit/receive beamforming pair. The exhaustive beam sweeping approach evaluates each beamforming pair by a number of metrics, such as the received power. Therefore, as the number of transmit/receive antennas and the size of the codebook continue to increase, the beam sweeping method will also incur prohibitive overhead [15].

It is worth remarking that the aforementioned beam alignment methods always require obtaining accurate and real-time CSI, which is extremely difficult for mmWave systems with limited RF links. Besides, these existing methods do not exploit prior local environment information that is specific to the locations of the receiver and transmitter, and this is a waste of valuable wireless environmental characteristics. Recently, a novel concept called *channel knowledge map*

(CKM) has been proposed in [19] in order to utilize prior local information of the actual wireless environment for the design and optimization of future communication systems. Specifically, CKM is a site-specific database, tagged with the locations of the transmitters and/or receivers, that provides location-specific channel knowledge useful to enhance environment-awareness and facilitate or even obviate sophisticated real-time CSI acquisition [19], [20]. Unlike physical environment maps [21], CKM can directly reflect the intrinsic channel characteristics that can be utilized for communication without the need for additional complex computations such as ray tracing. Meanwhile, compared to conventional radio environment maps (REMs) that mainly concern spectrum usage information [22], [23], CKM focuses on the location-specific wireless channel knowledge that is independent of the transmitter/receiver activities. Theoretical studies on CKM construction and utilization have received increasing attention recently. For example, the expectation-maximization algorithm is utilized in [24] to construct CKM by combining both expert knowledge about channel model and local measurement data, thus reducing the workload of the actual channel measurements. An environment-aware beam alignment scheme with CKM is proposed in [25], which utilizes a specific type of CKM, namely beam index map (BIM), to significantly reduce the computational cost and training overhead for real-time beamforming. The idea of using fingerprint maps like BIM to achieve beam alignment is similarly presented in [26]. CKM-based environment-aware beamforming approach was also studied for the IRS-aided communication [27].

Although theoretical studies have demonstrated the great potential of CKM-based environment-aware communication, to the best of our knowledge, no prototyping experimental studies have been conducted to verify the effectiveness of CKM in practical communication systems. To fill this gap, in this paper, we develop a prototyping experiment for CKM-based environment-aware communication for mmWave beam alignment. The main contributions of this work are summarized as follows:

- First, a general offline CKM construction method is presented. The method selects a typical type of CKM, called BIM, as an example, and explores the intrinsic relationship between channel information, location information and environment information. Specifically, the target area is divided into equidistant grids in accordance with the required precision. For each grid, the coordinates of its center are measured as the grid coordinates. An exhaustive beam sweeping is utilized to find the transmit and receive beam index pairs of each grid to complete the offline BIM construction. The proposed generic offline CKM construction method is applicable to both quasi-static and dynamic scenarios with line-of-sight (LoS) and non-line-of-sight (NLoS) links.
- A prototype of the CKM-based environment-aware mmWave communication system is completed through the integration of program design and hardware construction. The prototype consists of ultra-wide band (UWB) positioning module, mmWave phased array (mmPSA),

universal software radio peripheral (USRP), and gyroscope. During the communication process, the prototype obtains the stored channel knowledge such as LoS and NLoS links from the already built CKM based on the receiver's location to achieve training-free real-time mmWave beam alignment. The prototype also uses the orientation of the receiver from the gyroscope to refine and predict more accurate transmit and receive beam index pairings.

- Finally, the constructed CKM-based environment-aware mmWave communication prototype is experimentally verified. The performance of the CKM-based communication prototype is tested practically in a variety of quasi-static and dynamic scenarios. Compared with the exhaustive beam sweeping benchmark strategy, the CKM-based mmWave beam alignment strategy reduces the overhead from scanning 4096 beam index pairs to training-free. Furthermore, compared to the location-based beam alignment, the proposed CKM-based strategy obtains significantly greater received power in various scenarios. This demonstrates the feasibility and effectiveness of CKM for environment-aware mmWave communication.

The rest of this paper is organized as follows. Section II introduces the typical scenario of environment-aware communication that utilizes the CKM-based beam alignment strategy, and describes the theoretical basis of CKM. The hardware equipment and program design of the prototype are introduced in Section III. The construction of the CKM-based environment-aware mmWave communication prototype is specified in Section IV. Meanwhile, Section IV also shows the experimental results of the CKM-based beam alignment, and the comparison with the location-based benchmark is presented. Finally, the conclusion is drawn in Section V.

Notations: Scalars are denoted by italic letters. Vectors and matrices are denoted by boldface lower- and upper-case letters, respectively. $\mathbb{C}^{N \times M}$ denotes the space of $N \times M$ -dimensional complex-valued matrix. \mathbf{I}_N denotes an $N \times N$ identity matrix. For a matrix \mathbf{A} , its transpose, conjugate, Hermitian transpose, and determinant are respectively denoted as $\mathbf{A}^T, \mathbf{A}^*, \mathbf{A}^H$ and $|\mathbf{A}|$. For a vector \mathbf{a} , $[\mathbf{a}]_i$ denotes its i -th element. In addition, $\mathcal{CN}(\mu, \sigma^2)$ denotes the circularly symmetric complex Gaussian (CSCG) distribution with mean μ and variance σ^2 .

II. TYPICAL SCENARIO AND BASIC CONCEPTS

A. Communication Scenario

As shown in Fig. 1, we consider a typical mmWave massive MIMO communication scenario. A mmWave transmitter is located in the center of the considered area, and needs to serve three receivers. Considering the complexity of the communication environment, it is of great significance to select a suitable strategy to achieve beam alignment between the mmWave transmitter and receiver, thus enhancing the mmWave communication performance. Specifically, we first consider receiver 1 in Fig. 1. The LoS link with good channel conditions is available between the transmitter and receiver 1, and can be utilized for beam alignment and communication. Several strategies can be applied to obtain the optimal transmit

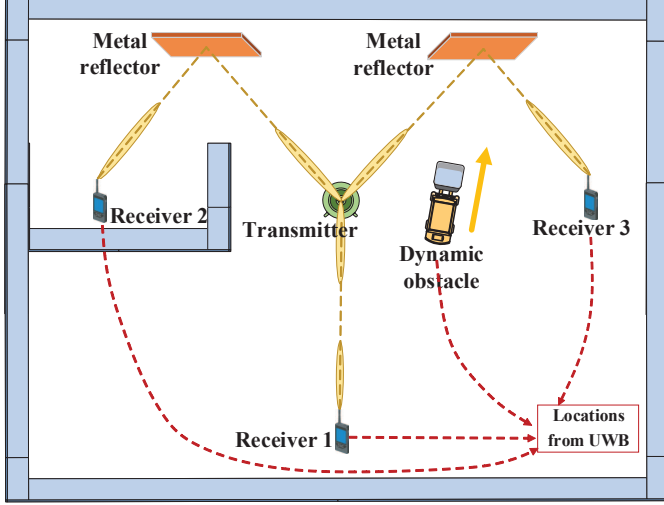


Fig. 1. A typical scenario for CKM-based environment-aware communication.

and receive beam pairs in this case, such as exhaustive beam sweeping, location-based beam calculation, and the proposed CKM-based beam alignment. Second, we consider the case of communication with receiver 2. Note that receiver 2 is located in a room with thick walls, which block the LoS link between the transmitter and receiver 2. The blocking of the LoS link renders the location-based beam calculation invalid, since it will lead to a beam pair directed to the LoS link. On the other hand, exhaustive beam sweeping and the CKM-based beam alignment can still find the strong reflected link provided by the metal reflector, thus enabling communication between the transmitter and receiver 2. For receiver 3, although there is no static blockage of the LoS link, a moving vehicle constitutes a dynamic obstruction in the communication environment. When the dynamic obstacle moves between receiver 3 and the transmitter, the LoS link is obstructed. In this situation, the location-based beam calculation can only provide the transmit and receive beam pair corresponding to the LoS link, resulting in poor performance. On the other hand, although exhaustive beam sweeping can switch the beam pair from the LoS link to the reflected link, it requires prohibitive delay and communication resources for sweeping all the possible beam pairs. Different from these two benchmark strategies, the CKM-based beam alignment switches the transmit and receive beam pair to the reflected link swiftly according to the location of the dynamic obstacles with the assistance of UWB positioning system to maintain the communication with the receiver 3.

B. Basic concept of CKM

CKM aims to provide the channel knowledge (such as path loss, angle-of-arrival (AoA)/angle-of-departure (AoD), beam indexes) based on location and orientation information of mobile devices and major obstacles, as illustrated in Fig. 2. Based on the acquired channel knowledge, the channel/beam can be reconstructed/selected directly, which is termed *CKM-based training-free communication* [19], [25], [27], [28].

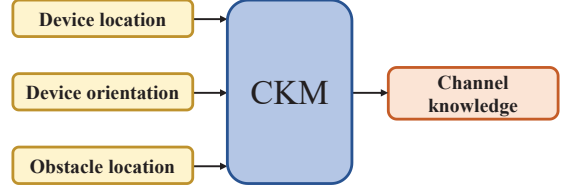


Fig. 2. An illustration of CKM for environment-aware communication.

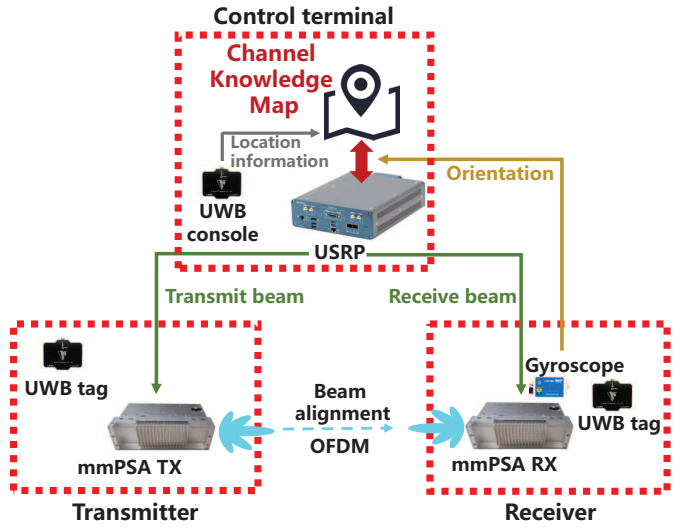


Fig. 3. The logical system for CKM-based mmWave wireless communication.

In this paper, we choose one specific type of CKM, named BIM, as an example in the experiment. Different from other types of CKM that store some specific channel knowledge such as gains, AOAs/AODs, etc., BIM directly stores several candidate indexes of transmit and receive beam pairs for each location of interest. With BIM, BS and UE can obtain candidate beam indexes based on their locations and implement refined beam sweeping within them, instead of exhaustively searching all the beam pairs. To construct the BIM, we divide the region of interest \mathcal{Q} into P small areas, denoted as $\mathbf{Q} = \{\mathcal{Q}_1, \dots, \mathcal{Q}_P\}$. BIM aims to learn the indexes of the possible beam pairs for all potential receiver locations \mathcal{Q}_p within the coverage of interest \mathcal{Q} , which can be expressed as

$$\text{BIM} : \{ \mathcal{Q}_p; (\hat{\mathcal{F}}_p, \hat{\mathcal{W}}_p) \}_{p=1}^P \quad (1)$$

where $\hat{\mathcal{F}}_p$ and $\hat{\mathcal{W}}_p$ are subset of the transmit and receive beam codebooks \mathcal{F} and \mathcal{W} , i.e., $\hat{\mathcal{F}}_p \subset \mathcal{F}, \hat{\mathcal{W}}_p \subset \mathcal{W}$, which have significantly reduced size $|\hat{\mathcal{F}}_p| \ll |\mathcal{F}|$ and $|\hat{\mathcal{W}}_p| \ll |\mathcal{W}|$.

Based on the real-time location information \mathbf{q} from the localization system, the area of the UE can be determined and the corresponding possible beam index pairs can be obtained from BIM. In BIM-based training-free communication, the beam index pair is selected for data transmission and reception, without additional real-time training.

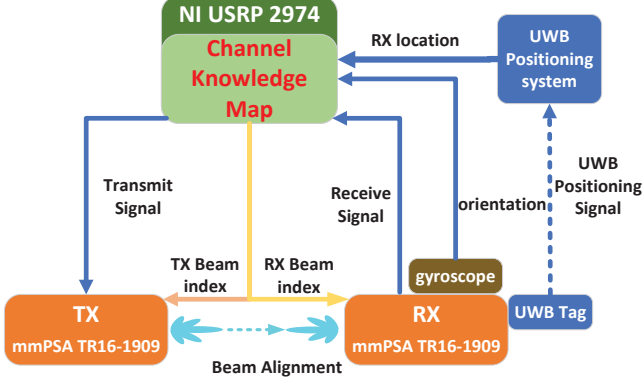


Fig. 4. The hardware system for implementing the CKM-based mmWave wireless communication.

III. PROTOTYPING EXPERIMENT IMPLEMENTATION

A. Prototype Architecture

The logical architecture of the prototyping system for CKM-based beam alignment is shown in Fig. 3, which is composed of the transmitter, the receiver, and the controller for CKM-based beam alignment by obtaining the receiver location information from the UWB positioning system and the receiver orientation from the gyroscope. The construction of CKM is completed offline in advance. In the process of online real-time communication, the system first obtains the location and orientation information of the receiver from the UWB positioning system and gyroscope, respectively. The controller determines in which grid the receiver is located according to the location information, and obtains the transmit beam corresponding to that grid directly according to the CKM constructed offline. Furthermore, the receive beam index is obtained based on both the receiver's location and orientation information. Finally, the transmit and receive beam indexes are forwarded to the transmitter and receiver, respectively, and the transmitter and receiver then complete beam alignment for communication by using the corresponding beam.

B. Hardware Equipment

As shown in Fig. 4, the hardware system is composed of four modules containing the NI USRP 2974 module for implementing the function of the controller, the mmPSA TR16-1909 module for mmWave phased antenna array, the UWB indoor positioning system, and the gyroscope module for obtaining the receiver's orientation.

1) *NI USRP 2974*: The NI USRP-2974 is a Software Defined Radio (SDR) stand-alone device built with a Field-Programmable Gate Array (FPGA) and an onboard processor for rapidly prototyping high-performance wireless communication systems. With a real time bandwidth of up to 160MHz, two daughter boards covering 10MHz to 6GHz are utilized to perform analog up/down conversion. The baseband signal sampling/interpolation and digital up/down conversion are realized rapidly on the Xilinx Kintex-7 410T FPGA, while the Intel i7 onboard processor is responsible for waveform related

operations like modulation/demodulation. Configured by the NI LabView Communication program, USRP-2974 can be operated as a transmitter to generate required signals flexibly and a receiver to process signals efficiently.

2) *mmPSA TR16-1909*: The mmPSA TR16-1909 is used as a phased antenna array for mmWave communication systems, which is a 16-element phased array and provides vertical polarization service. mmPSA TR16-1909 is cable-connected to USRP, to which the control frame is transmitted from the NI LabView Communications program to realize exhaustive beam sweeping. There are two control frame transmission methods, namely the SPI interface via HDMI line and the RS232 interface via USB-RJ45 connection line.

The device supports time division duplex (TDD) communication, whose operating frequency band is 27-29 GHz. The phase array provides the fast and normal modes in phase control. In the fast mode, 16 phase modules can be set independently, and the setting accuracy of each phase module is 5 bits. And in the normal mode, 16 phase modules are set simultaneously, and the setting accuracy is increased by 1 bit compared to the fast mode. The mmPSA TR16-1909 has a codebook with a scale of 64, where the angular range is from -56° to $+56^\circ$ in the horizontal direction.

3) *Nooploop UWB Indoor Positioning System*: The UWB indoor positioning system is used to measure the location of the receiver and transmitter in our experiment. The UWB technology can obtain Gbit/s data rate by transmitting nanosecond or shorter pulses. Compared with the traditional narrow-band system, the UWB system has superior anti-interference performance, a high transmission rate, an extremely wide bandwidth, a large system capacity, low transmission power, good confidentiality, etc. Therefore, it has obvious advantages in short-range high-speed data transmission and high-precision indoor positioning. The Nooploop UWB positioning system used in the CKM-based beam alignment prototype has a positioning update rate of 200Hz and a positioning accuracy of 10cm.

The UWB indoor positioning system is composed of the equipment layer, solution layer, and application layer, mainly including UWB base station, UWB tag, Power Over Ethernet (POE) switch, positioning engine, LabView program platform, etc. The main workflow is as follows: UWB tags are attached to the transmitter and receiver, sending the measurement signals to the base stations in the scenario through the UWB channel. In this experiment, five positioning base stations are set up, which collect tag data and transmit it to the solution engine in order to compute the UWB tag coordinates. After that, the parsed location information data is forwarded and uploaded to the LabView host computer and can be visualized in the LabView program platform, so as to control the mmPSA and perform CKM-based beam alignment based on the location information.

4) *Gyroscope Module*: The gyroscope module can efficiently obtain the real-time motion attitude with an attitude measurement accuracy of 0.2° and extremely high stability, which adopts a high-performance microprocessor and advanced dynamic filtering algorithm. It can provide real-time data with an update rate of up to 200Hz, so as to meet the

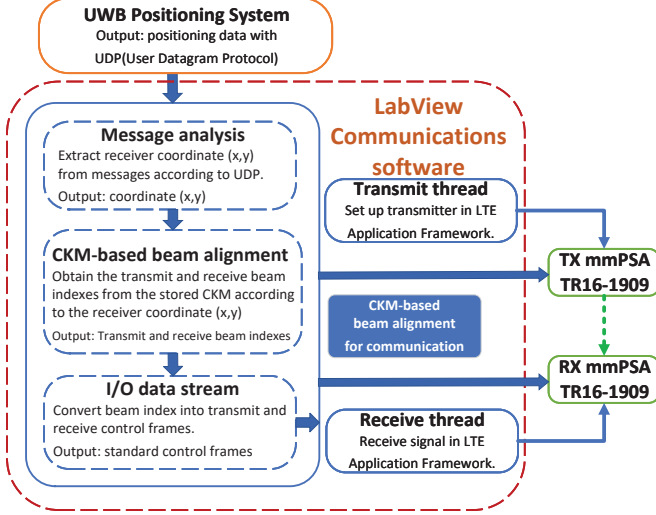


Fig. 5. The LabView communications program architecture for the CKM-based mmWave beam alignment prototype.

needs of various high-precision applications and accomplish accurate motion capture and attitude estimation.

C. Program Design

The experiments are conducted by using the LabView Communications program installed on the USRP 2974. The purpose of program design is to select the optimal beam index pair from the codebook of mmPSA to realize reliable real-time communication, when the location and orientation information of the receiver changes dynamically. As shown in Fig. 5, the designed program consists of three parallel primary threads: the transmit thread, the receive thread, and the CKM-based beam alignment thread.

In the designed program, the transmitter is always in the state of transmitting signals, and the quality of the received signal is then determined by observing the constellation diagram or the received power at the receiver. If the location or orientation information of the receiver changes significantly while the transmit and receive beam indexes remain unchanged, the received signal power can be observed to become lower and the constellation diagram becomes worse. Therefore, it is of paramount importance to select the optimal beam index pair in the CKM-based beam alignment thread to maintain high-quality communication. In the CKM-based beam alignment thread, the location data packets transmitted by the UWB positioning system are parsed to get the coordinate of the receiver first. Then, the transmit and receive beam indexes are obtained from the stored CKM according to the receiver's coordinate. Furthermore, the receive beam index is modified according to the orientation information of the receiver obtained from the gyroscope module. Finally, the transmit and receive beam indexes are converted into standard control frame format, which are sent to the transmit and receive mmPSA TR16-1909 via USB-RJ45 connection line, respectively.

IV. EXPERIMENTAL RESULTS

Prototyping experiments are conducted to demonstrate the environment-aware communication system with CKM-based beam alignment strategy. The common parameters of the experiments are listed as follows: 1) The selected mmPSAs are fully activated 16-antenna linear arrays. 2) The data transmission frequency of these prototypes is set as 28GHz. 3) Multiple modulation modes including QPSK, 16QAM, and 64QAM are used. In the experiments, the location-based beam alignment strategy is selected as the benchmark for comparison. The scenarios involved in the experiments include quasi-static and dynamic scenarios, and communication through both LoS and reflective NLoS links are considered.

A. Benchmark: Location-based Beam Alignment

The location-based beam alignment strategy generally assumes that there are no obstacles in the physical environment between the transmitter and the receiver. Therefore, this strategy considers the LoS link as the dominant link and performs beam alignment based on the LoS link. In the LoS case, the classical geometry-based channel model with a fixed transmitter can be written as

$$\mathbf{H}[t] = g(\mathbf{q}[t]) = \sqrt{M_r M_t} \gamma[t] \mathbf{a}_r(\theta_A[t]) \mathbf{a}_t^H(\theta_D[t]), \quad (2)$$

where $\mathbf{q}[t] = [q_x[t], q_y[t]]$ is the location of the receiver, $\gamma[t]$ is the complex gain of the LoS path, $\theta_A[t]$ and $\theta_D[t]$ are the AoA and AoD. Besides, $\mathbf{a}_t(\cdot)$ and $\mathbf{a}_r(\cdot)$ represent the transmit and receive array response vectors, respectively. In this case, the beam alignment problem is written as

$$\hat{\mathbf{f}}[t] = \arg \max_{\mathbf{f} \in \mathcal{F}} |\mathbf{a}_t^H(\theta_D[t]) \mathbf{f}|^2, \quad (3)$$

$$\hat{\mathbf{w}}[t] = \arg \max_{\mathbf{w} \in \mathcal{W}} |\mathbf{a}_r^H(\theta_A[t]) \mathbf{w}|^2, \quad (4)$$

where \mathbf{f} and \mathbf{w} are arbitrary beamforming vectors in the transmit and receive beam codebooks \mathcal{F} and \mathcal{W} , while $\hat{\mathbf{f}}$ and $\hat{\mathbf{w}}$ are the selected transmit and receive beamforming vectors, respectively.

For the location-based beam alignment strategy, location information is the key to performing beam alignment. This strategy mainly uses the receiver coordinate $[q_x[t], q_y[t]]$ and the transmitter coordinate $[b_x[t], b_y[t]]$ to calculate the angle $\phi[t]$ with respect to the x-axis, and then selects the transmit and receive beam index pair from the mmWave phased array codebook based on $\phi[t]$. According to the geometric relationship as shown in Fig. 6, the angle $\phi[t]$ between transmitter and receiver can be calculated as

$$\phi[t] = \arctan \left(\frac{q_y[t] - b_y[t]}{q_x[t] - b_x[t]} \right). \quad (5)$$

With the location-based beam alignment strategy, the corresponding prototype was built in a $4m \times 4m$ area. As shown in Fig. 7, two 16-antenna mmPSAs are used as receiver and transmitter, respectively. In the experimental area, there are five UWB base stations for positioning. UWB positioning tags are placed on the mmPSAs for real-time positioning of the transmitter and receiver. With the location information $\hat{\mathbf{b}}[t] = [\hat{b}_x[t], \hat{b}_y[t]]$ and $\hat{\mathbf{q}}[t] = [\hat{q}_x[t], \hat{q}_y[t]]$ obtained from the

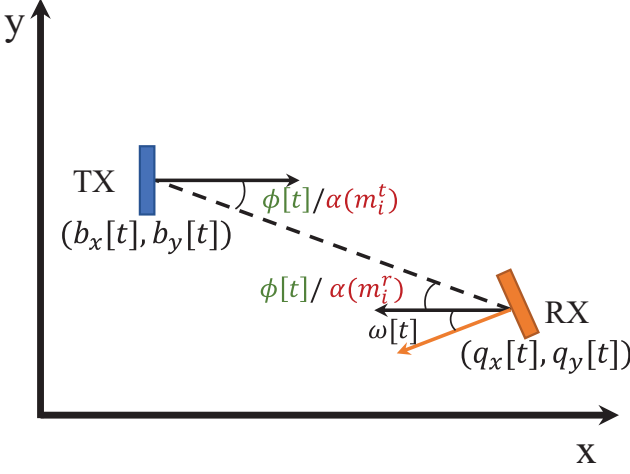
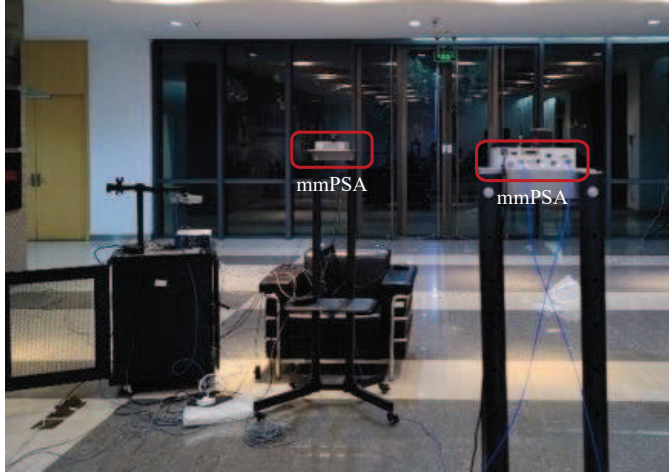


Fig. 6. A geometric illustration of the location/CKM-based beam alignment in LoS scenario.



(a)

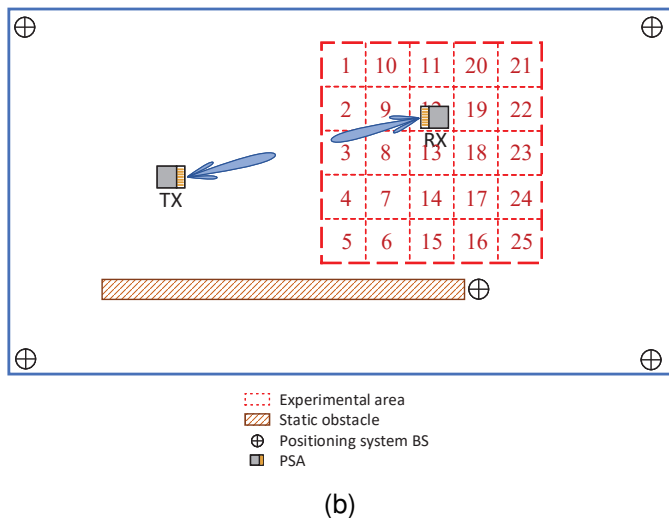


Fig. 7. CKM-based beam alignment with LoS link in quasi-static environment.

UWB module, the angle $\phi[t]$ will be calculated in real time. Further, with the receiver orientation $\omega[t]$ with respect to the

Algorithm 1 Process of the location-based beam alignment strategy

Input: The beam codebook $\{m, \alpha(m)\}$ of mmPSA, the angle $\phi[t]$ and the receiver orientation $\omega[t]$.

Output: The transmit and receive beam indexes i^* and j^* .

- 1: Initialization: Read the beam and pointing angle mapping codebook $\{m, \alpha(m)\}$.
- 2: **for** each time slot **do**
- 3: Obtain the location information of transmitter and receiver $\hat{\mathbf{b}}[t] = [\hat{b}_x[t], \hat{b}_y[t]]$ and $\hat{\mathbf{q}}[t] = [\hat{q}_x[t], \hat{q}_y[t]]$ from the UWB module.
- 4: Calculate the angle $\phi[t]$ between transmitter and receiver with (5).
- 5: Obtain the receiver orientation $\omega[t]$ from the gyroscope.
- 6: Calculate the transmit and receive beam indexes i^* and j^* with (6) and (7).
- 7: **end for**

x-axis acquired by the gyroscope on the receiver, the location-based strategy will refine the beam index at the receiver to obtain better beam alignment.

For mmPSAs at both the receiver and transmitter, the beam index and pointing angle mapping codebook has the following form as $\{m, \alpha(m)\}$, $m = 1, \dots, M$, where $\alpha(m)$ is the beam angle, denoting the angle between the beam center and the orientation of mmPSA, and m is the corresponding beam index. By calculating the angle $\phi[t]$ between the transmitter and receiver and obtaining the receiver orientation $\omega[t]$, the appropriate beam indexes can be found from the codebook. In this case, the transmit and receive beam indexes can be respectively selected as

$$i^* = \arg \min_i (|\phi[t] - \alpha(i)|), \quad (6)$$

$$j^* = \arg \min_j (|\phi[t] + \omega[t] - \alpha(j)|), \quad (7)$$

$$\hat{\mathbf{f}}[t] = h(i^*), \quad (8)$$

$$\hat{\mathbf{w}}[t] = h(j^*), \quad (9)$$

where h represents the conversion from beam index to preset beamforming vector in mmPSA. The detailed process of the location-based beam alignment strategy is summarized in Algorithm 1.

In order to avoid repeatedly sending the same control commands, we add a beam index detection process to the beam alignment scheme. Note that the selected beamforming vector $\hat{\mathbf{f}}[t]$ and $\hat{\mathbf{w}}[t]$ vary depending on the change in the position of the transmitter and receiver, not the time t . For example, if $\hat{\mathbf{f}}[t+1] = \hat{\mathbf{f}}[t]$, the beam index does not change and there is no need to send a PSA control command to the transmitter; if $\hat{\mathbf{f}}[t+1] \neq \hat{\mathbf{f}}[t]$, then the control frame should be sent to the transmitter to modify the beam index. The same applies to the receiver and its beamforming vector $\hat{\mathbf{w}}[t]$.

Fig. 7a and Fig. 7b show the actual scenario and the illustrative diagram of the location-based beam alignment

strategy, respectively. Although the location-based strategy is effective for LoS scenario depicted in Fig. 7a, it still needs to calculate the angle $\phi[t]$ between the receiver and transmitter in real time. Meanwhile, it is difficult for the location-based strategy to handle environments with blocked LoS link or dynamic environments. The above mentioned problems will be solved accordingly in the CKM-based beam alignment strategy.

B. CKM-based Beam Alignment in Quasi-Static Environment

In this section, a comparison will be made between the CKM-based beam alignment strategy and the location-based benchmark strategy in quasi-static environments. A typical LoS scenario and a typical NLoS scenario are selected, respectively. The corresponding CKMs are then constructed based on different environment information to help achieve beam alignment. The LoS scenario is identical to Fig. 7b, with the receiver orientation $\omega[t]$ changed arbitrarily. The NLoS scenario is shown in Fig. 8, where the orientation of the receiver is fixed with $\omega[t] = 0$ for simplicity. In Fig. 8, a concrete wall with a thickness of $0.4m$ exists between the transmitter and the receiver to block the LoS link. A copper reflector is placed to create reliable reflective link that can be utilized for communication.

1) *The construction of CKM*: In order to use environment information to help beam alignment, we fix the transmitter location and build a CKM for the area of interest for the receiver. In Fig. 7b, the CKM is built on a square area of size $4m \times 4m$, while in Fig. 8, the CKM is built on a square area of size $3.2m \times 4.8m$. The grid size is $0.8m \times 0.8m$. For each grid in CKM, the center coordinate is used as the grid's coordinate. In the offline construction of the CKM, the exhaustive beam sweeping method is used to determine the optimal beam index pairs. During the construction of CKMs, the receiver orientation is set to $\omega[t] = 0$. Considering that the construction steps of CKM are universal to LoS and NLoS scenarios, we take the NLoS scenario as an example and the specific process is as follows: First, the position of the transmitter is fixed, and the grids within the entire CKM are numbered from 1 to 24 in Fig. 8b. Then, the UWB tag is placed on the receiver, and the receiver is sequentially moved from grid 1 to grid 24 in sequence to find the optimal transmit and receive beam index pairs for the grid.

When the receiver moves to the center of grid i , the coordinate (x_i, y_i) of the receiver is obtained by the UWB system and stored in the CKM. After that, the beam index pair of the transmitter and receiver is switched to perform exhaustive beam sweeping. The difference between the diversified beam index pairs is reflected in the power of the signal received at the receiver. The higher the power of the received signal, the better the corresponding beam index pair. For each grid, communication tests with 64x64 beam index pairs are conducted, since each mmPSA has 64 preset beams in the codebook. The communication test for each beam pair lasts 30ms, during which the received signal power is read three times in 10ms intervals and the maximum received signal power is taken to reduce the impact of beam index pair

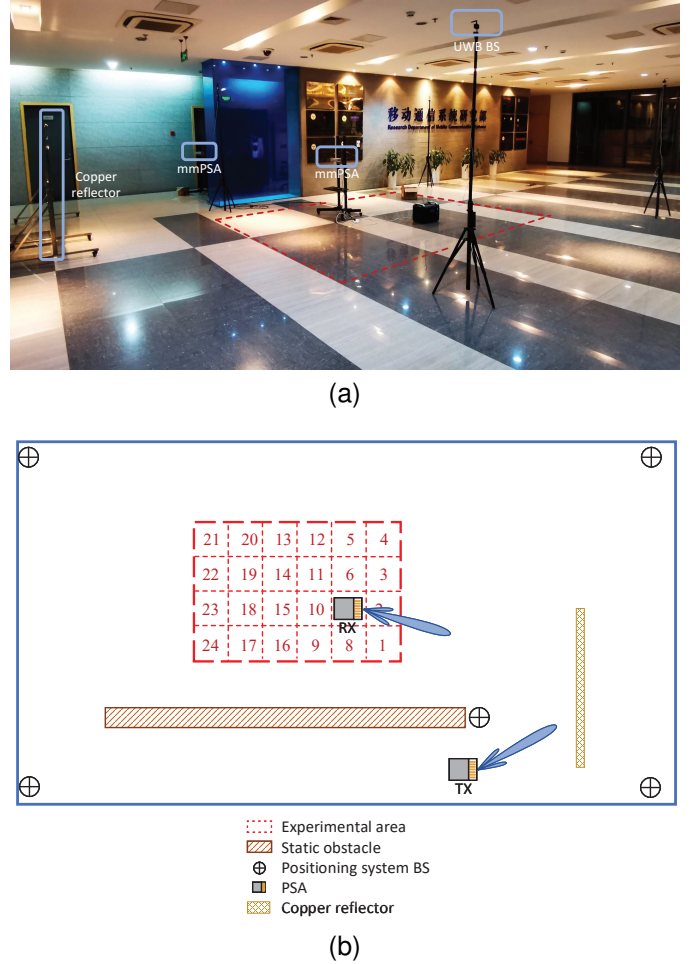


Fig. 8. CKM-based beam alignment with NLoS link in quasi-static environment.

switching on the communication performance. The transmit and receive beam index pair with the maximum received power will be selected and stored in the CKM as the optimal transmit and receive beam index pair (m_i^t, m_i^r) of the reflective NLoS link for grid i . Therefore, the corresponding CKM for grid i is recorded and saved in the following form as

$$c_i = \left\{ (x_i, y_i), (m_i^t, m_i^r) \right\}. \quad (10)$$

The complete CKM construction process of the CKM-based beam alignment is summarized in Algorithm 2. The construction step of the CKM does not change even in complex wireless environments, i.e., sweeping the transmit and receive beam pairs in the codebook. Therefore, when the number s_g of grids on the sides of a square area increases, which means the size of the environment increases, the construction complexity of the CKM is only $\mathcal{O}(s_c s_g^2)$, where s_c is the size of the codebook. This suggests that the complexity of construction does not depend on the complexity of the wireless environment.

2) *CKM experiment with LoS link*: In the static scenario with LoS link, the experiment with an arbitrary grid i in the CKM is conducted. The coordinates of the receiver are obtained by the UWB positioning system, while the orientation

Algorithm 2 General CKM construction process

Input: The beam codebook $\{m, \alpha(m)\}$ of mmPSA.
Output: The corresponding CKM $\{c_i\}$ for the grid.

- 1: Initialization: Fix the position of the transmitter, number the grids.
- 2: **for** each grid i **do**
- 3: Move the receiver to the center of grid i .
- 4: Obtain the receiver coordinate (x_i, y_i) by UWB.
- 5: **for** each transmit beam index **do**
- 6: **for** each receive beam index **do**
- 7: Conduct a communication test, record the received signal power at regular intervals,
- 8: Select the maximum received power from the three records for each beam index pair.
- 9: **end for**
- 10: **end for**
- 11: Select the optimal beam index pair (m_i^t, m_i^r) with the maximum received power.
- 12: Save the CKM for grid i as $c_i = \{(x_i, y_i), (m_i^t, m_i^r)\}$.
- 13: **end for**

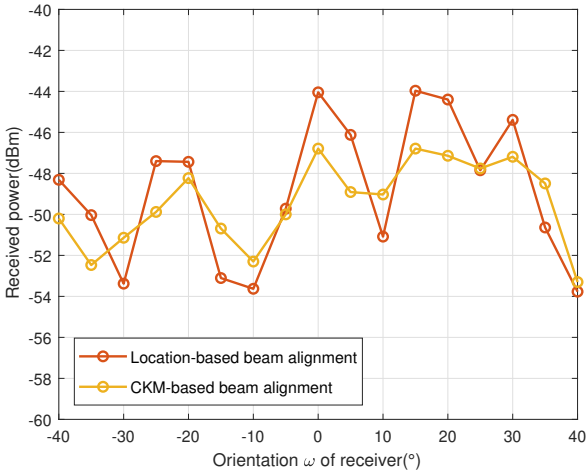


Fig. 9. Performance comparison of CKM-based and Location-based strategies under different receiver orientations.

$\omega[t]$ of the receiver is obtained by a gyroscope fixed on the receiver. The geometric representation of the CKM-based strategy in LoS scenario is also shown in Fig. 6. With continuously changing receiver orientation, the CKM-based beam alignment strategy can predict the transmit and receive beam pairs based on channel knowledge and receiver orientation. Specifically, the coordinate $\hat{\mathbf{q}}[t] = [\hat{q}_x[t], \hat{q}_y[t]]$ of the receiver can be obtained in real time through the UWB positioning system. By calculating the distance between the receiver and the center of each grid, we can find out which grid center is nearest to the real-time position of the receiver and thus determine which grid i^* the receiver is located in real time as

$$i^* = \arg \min_i \left((\hat{q}_x[t] - x_i)^2 + (\hat{q}_y[t] - y_i)^2 \right). \quad (11)$$

Then, the transmit beam index $m_{i^*}^t$ of grid i^* is obtained according to the constructed CKM, and the receive beam index is refined according to the receiver orientation $\omega[t]$ as

$$m_{i^*}^r = \arg \min_j \left(|\alpha(m_{i^*}^r) + \omega[t] - \alpha(j)| \right). \quad (12)$$

Fig. 9 shows the performance comparison of the two beam alignment strategies for different receiver orientations. The receiver orientation $\omega[t]$ ranges from -40° to 40° at the step of 5° . As can be seen from Fig. 9, for different receiver orientations, the CKM-based beam alignment strategy refines the beam index pairs read from the CKM according to orientation $\omega[t]$, and the received power obtained is very close to that of the location-based strategy. Therefore, the CKM-based beam alignment strategy is able to maintain good communication performance regardless of the orientation of the receiver. This is because the CKM-based strategy exploits the channel knowledge to first obtain the original transmit and receive beam index pairs stored in the CKM. Then the beam index pair is refined according to the receiver orientation to achieve good beam alignment. Therefore, in quasi-static scenarios with LoS links, the CKM-based beam alignment strategy can obtain comparable communication performance to the location-based benchmark strategy. The performance difference between the two strategies mainly comes from the location error and the gyroscope inertia error in different receiver orientations. The CKM-based strategy has smaller variation mainly because the location errors have a large impact on the location-based strategy, but generally do not interfere with the judgment of the nearest grid center, and therefore interfere less with the CKM-based strategy.

3) *CKM experiment with NLoS link:* The relevant information of the communication environment is embedded in the CKM $\{c_i\}$ and is expressed by the optimal beam index pair for each grid. During the experiment, the receiver can move freely within the constructed CKM area, while the prototype performs beam alignment through the already constructed CKM. For convenience, the receiver orientation is set to $\omega[t] = 0$. It is worth mentioning that the receiver orientation $\omega[t] = 0$ is assumed in order to demonstrate the beam alignment performance of the CKM-based strategy through NLoS links in different grids under uniform conditions. When $\omega[t] \neq 0$, the receive beam index read from the CKM should be refined according to $\omega[t]$, which is consistent with (12) in the LoS scenario. Specifically, the grid i^* to which the receiver belongs is first determined by the Euclidean distance of the receiver from each grid with (11). Similarly, the transmit beam index $m_{i^*}^t$ is obtained from the constructed CKM. Considering $\omega[t] = 0$ in (12), the index $m_{i^*}^r$ of grid i^* can be obtained directly from the CKM as the receiver beam index. A similar beam index detection process is added to the CKM-based beam alignment, i.e., the control frames are retransmitted only when the transmit or receive beam index changes.

The actual scenario and the illustrative diagram of the CKM-based beam alignment prototype are respectively shown in Fig. 8a and Fig. 8b. In Fig. 10, the communication performance of CKM-based beam alignment is compared with the benchmark location-based and beam sweeping strategies. As illustrated in

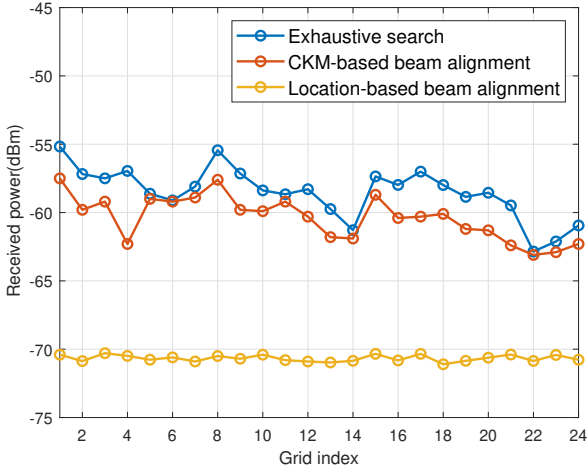


Fig. 10. Performance comparison between CKM-based and location-based strategies in NLoS scenario.

Fig. 10, the location-based strategy gives poor performance because it can only assume the LoS links that do not exist in the considered scenario. Meanwhile, since the reflective link considering the environment information is stored in the CKM in the form of beam index pairs, the CKM-based beam alignment strategy can use the reflective link for communication even if the LoS link is blocked. By comparing the received power at each grid, the CKM-based strategy is able to achieve a communication performance comparable to that of the exhaustive beam sweeping strategy, but with almost no real-time overhead. The modest performance loss is caused primarily by the receiver's location error relative to the grid center during movement.

C. CKM-based Beam Alignment in Dynamic Environment

CKM-based beam alignment is effective not only in quasi-static environments, but also in dynamic ones. In this experiment, a typical dynamic environment is considered, and the prototype's CKM-based beam alignment strategy is enhanced to increase the applicability of environment-aware communication. The experimental scenario is shown in Fig. 11a. The receiver maintains the fixed orientation with $\omega[t] = 0$. Meanwhile, a copper reflector is fixed on the side to simulate an NLoS link in a complex environment. Therefore, in this experimental scenario, both LoS and NLoS links may exist simultaneously. The communication link must be determined in real time based on the current condition of the dynamic environment. The UWB positioning system locates targets in the scenario by UWB tags. A $50\text{cm} \times 70\text{cm}$ small aluminum reflective plate is fixed on the moving vehicle to simulate the dynamic obstacles in the scenario. The moving vehicle is fitted with an auxiliary UWB tag to simulate dynamic obstacles.

1) *The construction of CKM*: The CKM in this experiment is built on a $4m \times 4m$ square area with $0.8m \times 0.8m$ grid. The process of CKM construction in a dynamic environment is similar to Algorithm 1. The main difference in the construction of CKM from Algorithm 1 is that, only the reflective

NLoS link in the environment is considered, i.e., the optimal beam index pair (m_i^t, m_i^r) needs to be found and stored in CKM. However, in the construction of CKM in the dynamic environment, both LoS and NLoS links need to be considered in order to improve the ability of the prototype to maintain communication in dynamic environments. Therefore, in the exhaustive search at each grid i , the optimal LoS link beam index pair (m_i^t, m_i^r) and reflective NLoS link beam index pair (l_i^t, l_i^r) need to be found out in the spatial direction according to the recorded received signal power and codebook, and stored in the corresponding CKM with the following format as

$$c_i = \{(x_i, y_i), (m_i^t, m_i^r), (l_i^t, l_i^r)\}. \quad (13)$$

2) *CKM experimental procedures and results*: The simulation of the dynamic environment and the process of CKM-based beam alignment in the corresponding dynamic environment are presented here. During the experiment, the moving vehicle with an aluminum reflective plate will serve as a significant communication environment-blocking dynamic obstacle. The receiver can communicate with the transmitter at any location within the constructed CKM area, and during the communication, we will move the moving vehicle to introduce dynamic blockage. The moving vehicle first moves toward the LoS link between transmitter and receiver, as in Fig. 11b. Considering that the LoS link is currently unimpeded, this phase is used to simulate a scenario where the dynamic environment does not affect communication temporarily. Next, we control the moving vehicle carrying an aluminum reflective plate across the LoS between the transmitter and receiver. As shown in Fig. 11c, the moving vehicle remains stationary for a period of time as it passes through the LoS link to simulate a scenario in which the LoS link is blocked. After that, the vehicle will continue to move until it is far away from the LoS link, which is used to represent the moment when the dynamic environment changes again and the LoS link recovers.

After obtaining the grid index, the key to CKM-based beam alignment in dynamic environments is determining which beam index pair in the CKM will be used for communication. Denote the real-time coordinate of the dynamic obstacle as $\hat{\mathbf{o}}[t] = [\hat{o}_x[t], \hat{o}_y[t]]$. In order to avoid the communication outage due to the dynamic obstacle, we use the distance-based judging rule to select the communication link. Specifically, the LoS link is used by default in the communication. Once the distance from the dynamic obstacle to the LoS link is less than a given threshold η , the selected communication link will switch from the LoS link to the reflective NLoS link in advance to avoid communication outage. To represent the position relation between dynamic obstacle and transmitter and receiver, we introduce the following vector according to the coordinates obtained from UWB positioning system

$$\begin{aligned} \overrightarrow{\text{TR}} &= \hat{\mathbf{q}}[t] - \hat{\mathbf{b}}[t] \\ &= [\hat{q}_x[t] - \hat{b}_x[t], \hat{q}_y[t] - \hat{b}_y[t]], \end{aligned} \quad (14)$$

$$\begin{aligned} \overrightarrow{\text{TO}} &= \hat{\mathbf{o}}[t] - \hat{\mathbf{b}}[t] \\ &= [\hat{o}_x[t] - \hat{b}_x[t], \hat{o}_y[t] - \hat{b}_y[t]], \end{aligned} \quad (15)$$

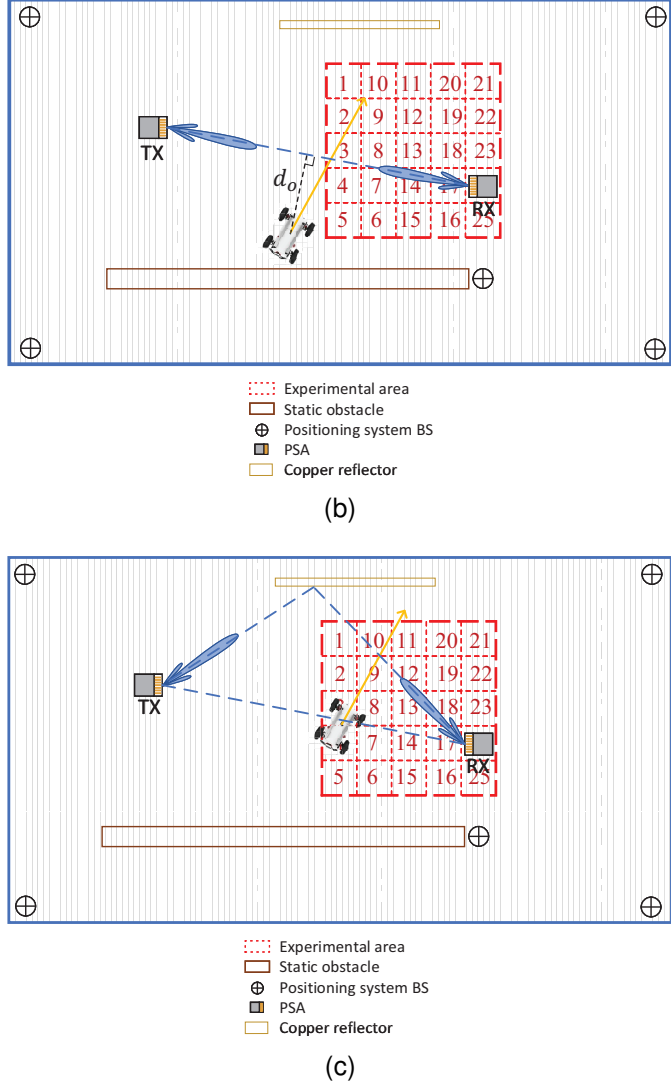


Fig. 11. CKM-based beam alignment in dynamic environment

where $\hat{\mathbf{b}}[t] = [\hat{b}_x[t], \hat{b}_y[t]]$, $\hat{\mathbf{q}}[t] = [\hat{q}_x[t], \hat{q}_y[t]]$ and $\hat{\mathbf{o}}[t] = [\hat{o}_x[t], \hat{o}_y[t]]$ denote the real-time coordinates of the transmitter, receiver and dynamic obstacle, respectively. $\overrightarrow{\text{TR}}$ represents the vector pointing from the transmitter to the receiver, while $\overrightarrow{\text{TO}}$ represents the vector pointing from the transmitter to the dynamic barrier.

As shown in Fig. 12, the ratio r of the length of the projection of $\overrightarrow{\text{TO}}$ on $\overrightarrow{\text{TR}}$ to the length of $\overrightarrow{\text{TR}}$ is calculated

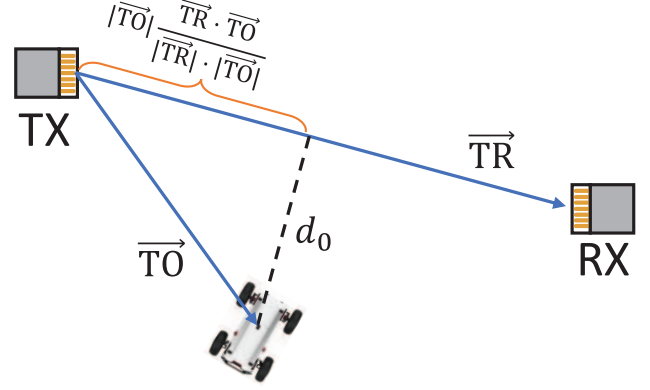


Fig. 12. A geometric illustration of the relationship between dynamic obstacle and devices.

Algorithm 3 CKM-based beam alignment process in dynamic environment

Input: The constructed CKM $\{c_i\}$ and the distance threshold η .

Output: The beam index pair $(m^t[n], m^r[n])$.

- 1: Initialization: obtain the real-time coordinates $\hat{\mathbf{b}}[t], \hat{\mathbf{q}}[t]$ and $\hat{\mathbf{o}}[t]$ from UWB.
- 2: Determine the grid i^* in CKM to which the receiver belongs by (11).
- 3: Calculate the ratio r with (16).
- 4: Calculate the distance d_o from the dynamic obstacle to the LoS link with (17).
- 5: **if** $0 < r < 1$ and $|d_o| \leq \eta$, **then**
- 6: $\hat{\mathbf{f}}[t] = h(m_{i^*}^t)$,
- 7: $\hat{\mathbf{w}}[t] = h(m_{i^*}^r)$,
- 8: **else**
- 9: $\hat{\mathbf{f}}[t] = h(l_{i^*}^t)$,
- 10: $\hat{\mathbf{w}}[t] = h(l_{i^*}^r)$.
- 11: **end if**

in (16), while the distance d_o from the dynamic obstacle to the LoS link is expressed as in (17)

$$r = \frac{|\overrightarrow{\text{TO}}| \frac{\overrightarrow{\text{TR}} \cdot \overrightarrow{\text{TO}}}{|\overrightarrow{\text{TR}}| \cdot |\overrightarrow{\text{TO}}|}}{|\overrightarrow{\text{TR}}|}, \quad (16)$$

$$|d_o| = |\overrightarrow{\text{TO}} - r\overrightarrow{\text{TR}}|. \quad (17)$$

A complete CKM-based beam alignment process in dynamic environments is shown in Algorithm 3.

In Fig. 13, we compare the performance of the CKM-based beam alignment with the benchmark location-based beam alignment in the dynamic environment. The received power is recorded versus different distances d_o from the dynamic obstacle to the LoS link with the step 10cm. Considering that half of the width of the aluminum reflective plate on the moving vehicle is 25cm, the distance threshold is set as $\eta = 30\text{cm}$. When the moving vehicle representing the dynamic obstacle just starts to move, it is far away from the LoS link, which is shown in Fig. 13 with $-50\text{cm} \leq d_o < -30\text{cm}$. In this case, the LoS link is almost undisturbed by the dynamic

obstacle, and the CKM-based beam alignment strategy chooses the LoS link with (m_i^t, m_i^r) for communication, which is consistent with the results obtained by the location-based strategy. This explains the coincidence of the two received power lines with $-50\text{cm} \leq d_o < -30\text{cm}$. When $-30\text{cm} \leq d_o \leq 30\text{cm}$, which means $|d_o| < \eta$, different beam index pairs are selected for communication by the benchmark location-based and the CKM-based strategies. On the one hand, the location-based strategy has no knowledge of the dynamic environment and can only choose the beam index pair of the LoS link. Thus, as the distance d_o changes from -30cm to 30cm , the LoS link is first gradually obstructed by the dynamic obstacle and then gradually recovers, which also leads to a decrease and then an increase in the received power and a corresponding minimum at $d_o = 0\text{cm}$. On the other hand, the CKM-based beam alignment strategy fully considers the impact of dynamic obstacle and switches to NLoS beam index pair (l_i^t, l_i^r) in time ($|d_o| \leq \eta$). When the CKM-based strategy switches to the NLoS link for communication, the corresponding received power has a power loss up to 5dB , which corresponds to the path loss between the alternative NLoS link and the LoS link. Compared with the location-based strategy, the resulting gain of the received power is up to 8dB or more. This fully demonstrates that the CKM-based beam alignment can effectively cope with the variation of environment and improve communication performance through pre-stored channel knowledge. Notice that the location-based strategy performs better at $d_o = 30\text{cm}$. This can be explained by the spatial limitations of the experimental site, where the dynamic obstacle moves closer to the copper reflector as the moving vehicle moves, thereby impacting the NLoS link and diminishing its performance to some degree. As the distance increases to $d_o \geq 30\text{cm}$, the CKM-based strategy treats the impact of dynamic obstacle on the LoS link as negligible and switches the beam index pair back to the LoS link (m_i^t, m_i^r) . Therefore, the curves of the received power are once again consistent for both the benchmark and the CKM-based beam alignment.

V. CONCLUSION

In this paper, a prototype system is developed for CKM-based environment-aware mmWave beam alignment. CKM makes full use of the prior information about the actual environment to build a database that effectively reflects channel knowledge, thus enabling training-free environment-aware beam alignment. We first set up a general offline CKM construction method. Then, by hardware integration and program design, a CKM-based mmWave beam alignment environment-aware communication prototype is built. The communication performance of the CKM-based beam alignment strategy is compared with the location-based benchmark strategy under various quasi-static and dynamic scenarios, effectively revealing the effectiveness and feasibility of the CKM-based mmWave beam alignment system.

REFERENCES

[1] S. Mumtaz, J. Rodriguez, and L. Dai, *MmWave massive MIMO: A paradigm for 5G*. Academic Press, ISBN:9780128044186, 2016.

[2] R. W. Heath, N. Gonzalez-Prelicic, S. Rangan, W. Roh, and A. M. Sayeed, "An overview of signal processing techniques for millimeter wave MIMO systems," *IEEE J. Sel. Topics Signal Process.*, vol. 10, no. 3, pp. 436–453, Apr. 2016.

[3] T. S. Rappaport, S. Sun, R. Mayzus, H. Zhao, Y. Azar, K. Wang, G. N. Wong, J. K. Schulz, M. Samimi, and F. Gutierrez, "Millimeter wave mobile communications for 5G cellular: It will work!" *IEEE Access*, vol. 1, pp. 335–349, 2013.

[4] X. Zhang, A. Molisch, and S.-Y. Kung, "Variable-phase-shift-based rf-baseband codesign for MIMO antenna selection," *IEEE Trans. Signal Process.*, vol. 53, no. 11, pp. 4091–4103, Nov. 2005.

[5] V. Venkateswaran and A.-J. van der Veen, "Analog beamforming in MIMO communications with phase shift networks and online channel estimation," *IEEE Trans. Signal Process.*, vol. 58, no. 8, pp. 4131–4143, Aug. 2010.

[6] O. E. Ayach, S. Rajagopal, S. Abu-Surra, Z. Pi, and R. W. Heath, "Spatially sparse precoding in millimeter wave MIMO systems," *IEEE Trans. Wirel. Commun.*, vol. 13, no. 3, pp. 1499–1513, Mar. 2014.

[7] A. Alkhateeb, O. El Ayach, G. Leus, and R. W. Heath, "Channel estimation and hybrid precoding for millimeter wave cellular systems," *IEEE J. Sel. Topics Signal Process.*, vol. 8, no. 5, pp. 831–846, Oct. 2014.

[8] A. Alkhateeb, J. Mo, N. Gonzalez-Prelicic, and R. W. Heath, "MIMO precoding and combining solutions for millimeter-wave systems," *IEEE Commun. Mag.*, vol. 52, no. 12, pp. 122–131, Dec. 2014.

[9] Y. Zeng and R. Zhang, "Millimeter wave MIMO with lens antenna array: A new path division multiplexing paradigm," *IEEE Trans. Commun.*, vol. 64, no. 4, pp. 1557–1571, Apr. 2016.

[10] X. Gao, L. Dai, S. Han, C.-L. I, and X. Wang, "Reliable beamspace channel estimation for millimeter-wave massive MIMO systems with lens antenna array," *IEEE Trans. Wirel. Commun.*, vol. 16, no. 9, pp. 6010–6021, Sep. 2017.

[11] Y. Zeng and R. Zhang, "Cost-effective millimeter-wave communications with lens antenna array," *IEEE Wirel. Commun.*, vol. 24, no. 4, pp. 81–87, Aug. 2017.

[12] J. Yang, Y. Zeng, S. Jin, C.-K. Wen, and P. Xu, "Communication and localization with extremely large lens antenna array," *IEEE Trans. Wirel. Commun.*, vol. 20, no. 5, pp. 3031–3048, May. 2021.

[13] J. Lee, G.-T. Gil, and Y. H. Lee, "Channel estimation via orthogonal matching pursuit for hybrid MIMO systems in millimeter wave communications," *IEEE Trans. Commun.*, vol. 64, no. 6, pp. 2370–2386, Jun. 2016.

[14] K. Venugopal, A. Alkhateeb, N. G. Prelicic, and R. W. Heath, "Channel estimation for hybrid architecture-based wideband millimeter wave systems," *IEEE J. Sel. Areas Commun.*, vol. 35, no. 9, pp. 1996–2009, Sep. 2017.

[15] M. Giordani, M. Polese, A. Roy, D. Castor, and M. Zorzi, "A tutorial on beam management for 3GPP NR at mmWave frequencies," *IEEE Commun. Surv. Tutor.*, vol. 21, no. 1, pp. 173–196, Sep. 2018.

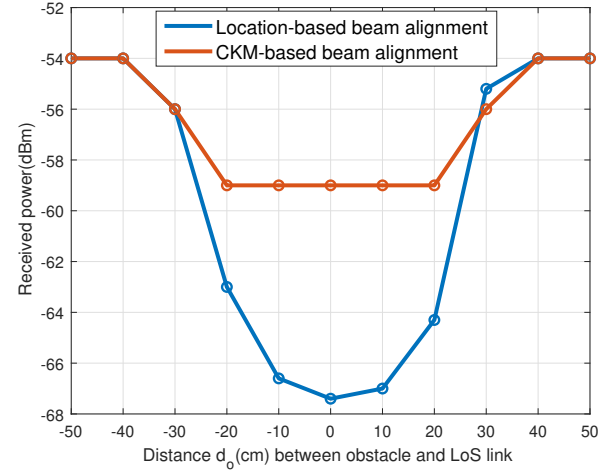


Fig. 13. Performance comparison between CKM-based and location-based strategies in dynamic environment.

- [16] Y. Heng, J. G. Andrews, J. Mo, V. Va, A. Ali, B. L. Ng, and J. C. Zhang, "Six key challenges for beam management in 5.5G and 6G systems," *IEEE Commun. Mag.*, vol. 59, no. 7, pp. 74–79, Jul. 2021.
- [17] J. Kim, "Elements of next-generation wireless video systems: Millimeter-wave and device-to-device algorithms," Ph.D. dissertation, University of Southern California, 2014.
- [18] J. Kim and A. F. Molisch, "Fast millimeter-wave beam training with receive beamforming," *J. Commun. Networks.*, vol. 16, no. 5, pp. 512–522, 2014.
- [19] Y. Zeng and X. Xu, "Toward environment-aware 6G communications via channel knowledge map," *IEEE Wireless Commun.*, vol. 28, no. 3, pp. 84–91, Jun. 2021.
- [20] Y. Zeng, J. Chen, J. Xu, D. Wu, X. Xu, S. Jin, X. Gao, D. Gesbert, S. Cui, and R. Zhang, "A tutorial on environment-aware communications via channel knowledge map for 6G," *accepted by IEEE Commun. Surv. Tutor.* [Online]. Available: <https://arxiv.org/abs/2309.07460>.
- [21] S. Y. Seidel and T. S. Rappaport, "Site-specific propagation prediction for wireless in-building personal communication system design," *IEEE Trans. Veh. Technol.*, vol. 43, no. 4, pp. 879–891, Nov. 1994.
- [22] H. B. Yilmaz, T. Tugcu, F. Alagöz, and S. Bayhan, "Radio environment map as enabler for practical cognitive radio networks," *IEEE Commun. Mag.*, vol. 51, no. 12, pp. 162–169, Dec. 2013.
- [23] S. Bi, J. Lyu, Z. Ding, and R. Zhang, "Engineering radio maps for wireless resource management," *IEEE Wirel. Commun.*, vol. 26, no. 2, pp. 133–141, 2019.
- [24] K. Li, P. Li, Y. Zeng, and J. Xu, "Channel knowledge map for environment-aware communications: Em algorithm for map construction," in *Proc. IEEE Wireless Commun. Netw. Conf (WCNC)*. IEEE, 2022, pp. 1659–1664.
- [25] D. Wu, Y. Zeng, S. Jin, and R. Zhang, "Environment-aware hybrid beamforming by leveraging channel knowledge map," *IEEE Trans. Wirel. Commun.*, pp. 1–1, 2023.
- [26] V. Va, J. Choi, T. Shimizu, G. Bansal, and R. W. Heath, "Inverse multipath fingerprinting for millimeter wave V2I beam alignment," *IEEE Trans. Veh. Technol.*, vol. 67, no. 5, pp. 4042–4058, May. 2018.
- [27] D. Ding, D. Wu, Y. Zeng, S. Jin, and R. Zhang, "Environment-aware beam selection for IRS-aided communication with channel knowledge map," in *Proc. IEEE Global Commun. Conf. (GLOBECOM) Workshops*. IEEE, 2021, pp. 1–6.
- [28] D. Wu, Y. Zeng, S. Jin, and R. Zhang, "Environment-aware and training-free beam alignment for mmWave massive MIMO via channel knowledge map," in *Proc. IEEE Int. Conf. Commun. (ICC)*. IEEE, 2021, pp. 1–7.